



Jin Sheng Du  
Associate Professor, School of Civil Engineering, Beijing Jiao Tong University, Beijing, China



Francis T. K. Au  
Associate Professor, Department of Civil Engineering, The University of Hong Kong, China

## Estimation of ultimate stress in external FRP tendons

J. S. DU MS, PhD and F. T. K. Au MSc(Eng), PhD, CEng, MICE, FStructE, MHKIE

**In a prestressed concrete beam with external tendons, the tendon stress depends on the member deformation, and it cannot be determined from section analysis alone as in the bonded case. Previous work has been mainly on the ultimate stress in unbonded steel tendons, with little on unbonded fibre-reinforced polymer (FRP) tendons. To account for the relative slip between the unbonded tendon and concrete, the ratio of the equivalent plastic hinge length to the neutral axis depth is analysed using available test results. It is found that this ratio for unbonded partially prestressed concrete (UPPC) beams with external FRP tendons can also be treated as a constant as for those with unbonded steel tendons. A simple method for evaluation of the ultimate stress in either steel or FRP external tendons is therefore proposed. After suitable modifications, the equations currently adopted by various design codes can still be used to predict the ultimate stress in external FRP tendons of UPPC beams.**

### NOTATION

$A_p$	cross-sectional area of tendons
$A_s, A'_s$	cross-sectional areas of tension and compression for non-prestressed steel respectively
$b, b_w$	widths of flange and web respectively
$c$	neutral axis depth
$C_f$	compressive force carried by flange
$d_p$	depth to centroid of tendons
$E_p$	Young's modulus of tendons
$E_{\text{steel}}, E_{\text{FRP}}$	Young's moduli of steel and FRP tendons respectively
$f$	coefficient dependent on loading type
$f'_c$	cylinder compressive strength of concrete
$f_{pe}$	effective prestress in tendons
$f_{ps}$	ultimate stress in unbonded steel or FRP tendons at failure of member
$\Delta f_{ps}$	tendon stress increment at ultimate
$f_{py}, f_{pu}$	yield and ultimate strength of tendons respectively
$f_y, f'_y$	yield stresses of tension and compression for non-prestressed steel respectively
$h_f$	thickness of flange
$L$	length of unbonded tendons between end anchorages
$L_n$	span of beam
$L_p$	equivalent plastic hinge length

$N$	number of support hinges required to form a failure mechanism crossed by the tendon
$q_0$	combined reinforcement index
$\epsilon_{cu}$	ultimate compressive strain in concrete
$\theta$	rotation of plastic hinge
$\varphi$	ratio of equivalent plastic hinge length to neutral axis depth
$\Omega_u$	bond reduction coefficient

### 1. INTRODUCTION

The use of external prestressing not only leads to simple and economical designs but also enables fast installation and easy replacement of defective tendons. External tendons can be made of high-strength steel or fibre-reinforced polymers (FRP), such as carbon fibre-reinforced polymers (CFRP), aramid fibre-reinforced polymers (AFRP) and glass fibre-reinforced polymers (GFRP). Because of the lack of bonding between the tendons and concrete, the tendon stress upon loading depends on the member deformation, and it cannot be determined from section analysis alone as in the bonded case. Many studies had been carried out within the past five decades for prediction of flexural resistance of prestressed concrete (PC) beams with unbonded tendons, which was closely related to the ultimate tendon stress  $f_{ps}$  at failure. Most of the equations suggested for  $f_{ps}$  are, however, based on steel tendons and may not apply to FRP tendons without validation.

The ratio  $\varphi$  of the equivalent plastic hinge length to the neutral axis depth is analysed using test results of three groups, including the unbonded partially prestressed concrete (UPPC) beams with external CFRP tendons in Beijing Jiao Tong University,<sup>1</sup> the UPPC beams with external AFRP tendons in The University of Hong Kong<sup>2</sup> and those of Ghallab and Beeby.<sup>3</sup> Values of the parameter  $\varphi$  for UPPC beams with external FRP tendons are then compared with those for UPPC beams with unbonded steel tendons, with a view to devising a consistent method for evaluation of the ultimate tendon stress.

### 2. REVIEW OF PREVIOUS WORK

Comprehensive reviews of the ultimate stress in unbonded tendons at flexural failure were reported by Naaman and Alkhaiir,<sup>4</sup> Allouche *et al.*<sup>5</sup> and Au and Du.<sup>6</sup> Various groups have also come up with improved methods, and some of the design formulae have been adopted in various codes. The equations fall into two main categories: the bond reduction coefficient approach and the deformation-based approach. Naaman and

Alkhairi<sup>7</sup> have proposed an equation based on the bond reduction coefficient for the ultimate tendon stress  $f_{ps}$ , namely

$$1 \quad f_{ps} = f_{pe} + \Omega_u E_p \epsilon_{cu} \left( \frac{d_p}{c} - 1 \right) \frac{L_1}{L_2} \leq 0.94 f_{py} \text{ (MPa)}$$

where the bond reduction factor is taken as  $\Omega_u = k/(L/d_p)$ ,  $L_1/L_2$  is the ratio of the length of loaded span(s) in continuous members to the total length of tendon between anchorages,  $d_p$  is the depth to centroid of tendons,  $f_{pe}$  and  $f_{py}$  are the effective prestress and yield strength of tendon respectively,  $E_p$  is the Young's modulus of tendon,  $\epsilon_{cu}$  is the ultimate concrete compression strain equal to 0.003,  $k$  is the load type factor and  $c$  is the neutral axis depth. Based on the experimental data,  $k$  is found to be 2.6 for mid-span loading and 5.4 for third-point loading. For design purposes, the values of  $k$  are reduced to 1.5 and 3.0, respectively.

The unknowns  $c$  and  $f_{ps}$  in Equation 1 can be solved from the equilibrium equations

$$2a \quad A_p f_{ps} + A_s f_y - A'_s f'_y = 0.85 \beta_1 f'_c b_w c + C_f \text{ (N)}$$

$$2b \quad \begin{cases} C_f = 0.85 \beta_1 f'_c (b - b_w) h_f & \text{if } \beta_1 c > h_f \\ C_f = 0, b_w = b & \text{if } \beta_1 c \leq h_f \end{cases}$$

$$2c \quad \begin{cases} \beta_1 = 0.85 & \text{if } f'_c < 28 \text{ MPa} \\ \beta_1 = 0.85 - 0.05(f'_c - 28)/7 & \text{if } 28 \text{ MPa} \leq f'_c \leq 56 \text{ MPa} \\ \beta_1 = 0.65 & \text{if } f'_c > 56 \text{ MPa} \end{cases}$$

where  $A_p$  is the cross-sectional area of tendon,  $A_s$  and  $f_y$  are respectively the cross-sectional area and yield strength of ordinary tension reinforcement,  $A'_s$  and  $f'_y$  are respectively the cross-sectional area and yield strength of compression reinforcement,  $f'_c$  is the cylinder compressive strength of concrete,  $b$  and  $b_w$  are respectively the breadths of flange and web,  $h_f$  is the thickness of top flange,  $C_f$  is the compressive force carried by the flange if applicable, and  $\beta_1$  is the concrete compression block reduction factor.

Naaman *et al.*<sup>8</sup> further modified Equation 1 for steel or FRP tendons, and recommended two equations for the ultimate tendon stress at flexural failure. Ghallab and Beeby<sup>9</sup> also revised the bond reduction factor  $\Omega_u$  in Equation 1 taking into account the internal bonded non-prestressed steel and external FRP tendons. Ng<sup>10</sup> suggested a modified bond reduction coefficient independent of the span–depth ratio while accounting for the second-order effect of external tendons.

The bond reduction method of Naaman and Alkhairi, namely Equation 1, was adopted in the 1994 version of the AASHTO LRFD Bridge Code,<sup>11</sup> but the equation was replaced by a deformation-based equation in the 1998 version.<sup>12</sup> As pointed out by Au and Du,<sup>6</sup> Equation 1 is heavily influenced by the load type. For example, the value of  $k$  for mid-span loading is about half that for third-point loading. It is also affected by the arrangement of spans that are loaded. For the ultimate limit state of a highway bridge for instance, it is difficult to judge if

one-point or third-point loading should be chosen, and so is the choice of loading arrangements in multi-span beams.

In the deformation-based approach, the beam deformation is assumed to be concentrated in the length of equivalent plastic hinge  $L_p$ , and all unbonded tendon elongation is considered to come from the region of equivalent plastic hinge. There are two schools of thought on the determination of equivalent plastic hinge length  $L_p$ . The estimate of equivalent plastic hinge length  $L_p$  introduced by Harajli<sup>13</sup> gives

$$3 \quad L_p = \frac{L}{f} + 0.5d_p + 0.05Z \text{ (mm)}$$

where  $Z$  is the shear span,  $f$  is a coefficient dependent on the loading type and  $L$  is the length of unbonded tendons between anchorages. The coefficient  $f$  may take different values, namely  $f = \infty$  for single concentrated load,  $f = 3$  for two third-point concentrated loads and  $f = 6$  for uniform loading.

The other approach is to relate  $L_p$  to the neutral axis depth  $c$ , namely  $L_p = \phi c$ , where the parameter  $\phi$  is the ratio of equivalent plastic hinge length to neutral axis depth. It was originally put forward by Pannell,<sup>14</sup> and developed by Tam and Pannell.<sup>15</sup> After analysis of test results from various sources, Au and Du<sup>16</sup> observed that Harajli's  $L_p$  model placed much emphasis on the effects of loading type on stress increment in unbonded tendons at flexural failure of the beam. In Pannell's  $L_p$  model, the parameter  $\phi$  is stable and can be treated as constant. Recently, Roberts-Wollmann *et al.*<sup>17</sup> presented an equation for the ultimate stress in external tendons that was adopted by the current AASHTO LRFD Code<sup>12</sup> and AASHTO Segmental Bridge Specifications.<sup>18</sup> The equation is actually based on Pannell's model with  $\phi$  taken as 10.5. In assessment of the equation of Roberts-Wollmann *et al.*, Harajli<sup>19</sup> gave reasons for scatter in prediction of ultimate stress increase in unbonded tendons, and analysed the measured values of  $L_p$  for 176 specimens from different investigators. He also observed that whenever the values of  $L_p$  were plotted as a linear function of the neutral axis depth  $c$ , as proposed by Pannell,<sup>14</sup> and Tam and Pannell,<sup>15</sup> the trend became clearer. He suggested a revised equation for  $L_p$ , incorporating the neutral axis depth  $c$  and load type  $f$ , as

$$4 \quad L_p = \left( \frac{20.7}{f} + 10.5 \right) c \text{ (mm)}$$

where  $f = \infty$  for single concentrated load,  $f = 3$  for two third-point loads and  $f = 6$  for uniform loading, and  $L$  is the length of unbonded tendons between anchorages.

There are certain problems in incorporating the load type into the calculation of  $L_p$ . Investigators have not yet reached a consensus about the load type effect on the ultimate stress in unbonded tendons. It is also difficult to determine the load type at ultimate limit state for structures such as highway bridges. The test data of Harajli and Kanj<sup>20</sup> indicated that the stress increase in unbonded tendons at ultimate was not consistently higher for beams with mid-span loading compared to beams with third-point loading. From analysis of these data,

it is also found that the experimental values of  $L_p$  for members under mid-span loading are comparable in magnitude to their counterparts tested under third-point loading.<sup>16</sup>

Pannell's deformation-based model for determination of the ultimate stress  $f_{ps}$  in unbonded tendons also formed the basis of the British Code BS 8110,<sup>21</sup> the Canadian Code A23.3-94,<sup>22</sup> and the draft Chinese Code for Strengthening of Highway Bridges.<sup>23</sup> Although the above codes, together with the AASHTO LRFD and AASHTO Segmental Bridge Codes, are all based on Pannell's model, there are some differences in the values of parameter  $\varphi$ , calculation of neutral axis depth  $c$ , and how to account for the effect of continuous beams.

### 3. FURTHER DEVELOPMENT OF DEFORMATION-BASED MODEL

According to Pannell's deformation-based model, the failure of a UPPC beam can be modelled as a series of rigid members connected by plastic hinges at critical sections, as shown in Figure 1. If the rotation of the plastic hinge is denoted by, and the distance from the neutral axis to the tendon is  $z_p = d_p - c$ , then the tendon elongation can be written as<sup>17</sup>

$$5 \quad \delta = z_p \theta = (d_p - c) \theta \quad (\text{mm})$$

The corresponding tendon strain increase is

$$6 \quad \Delta \epsilon_{ps} = \frac{\delta}{L} = \frac{(d_p - c) \theta}{L}$$

where  $L$  is the length of unbonded tendons between anchorages. From strain considerations, the rotation of the plastic hinge can be approximated as

$$7 \quad \theta = L_p \frac{\epsilon_{cu}}{c}$$

According to Pannell,<sup>14</sup> and Tam and Pannell,<sup>15</sup> the ratio of equivalent plastic hinge length  $L_p$  to neutral axis depth  $c$ , namely  $\varphi = L_p/c$ , can be treated as a constant for PC beams with unbonded tendons even for different span/depth ratios. Assuming the unbonded tendons to remain elastic and further making use of Equations 6 and 7, the tendon stress at ultimate  $f_{ps}$  appears as

$$8 \quad \begin{aligned} f_{ps} &= f_{pe} + \Delta f_{ps} = f_{pe} + E_p \Delta \epsilon_{ps} \\ &= f_{pe} + \frac{\varphi E_p \epsilon_{cu} (d_p - c)}{L} \quad (\text{MPa}) \end{aligned}$$

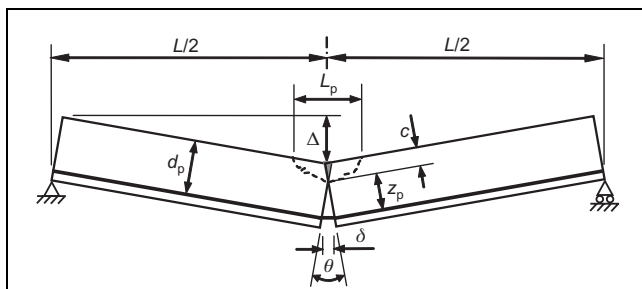


Figure 1. Assumed failure mechanism of a simply supported UPPC beam

where  $\Delta f_{ps}$  is the tendon stress increment at ultimate.

In the AASHTO LRFD Code<sup>12</sup> and AASHTO Segmental Bridge Code,<sup>18</sup> the associated parameters are:  $\varphi = 10.5$ ,  $\epsilon_{cu} = 0.003$  and  $E_p = 200 \text{ kN/mm}^2$ , giving  $\varphi E_p \epsilon_{cu} = 6300 \text{ N/mm}^2$ . The tendon stress at ultimate  $f_{ps}$  is

$$9 \quad f_{ps} = f_{pe} + \frac{6300 (d_p - c)}{l_c} \quad (\text{MPa})$$

where  $l_c = L/(1 + N/2)$ ,  $L$  is the length of tendon between anchorages or fully bonded deviators, and  $N$  is the number of support hinges required to form a failure mechanism crossed by the tendon.

Eliminating the neutral axis depth  $c$  between Equation 8 and Equations 2a to 2c for equilibrium at the critical section, a general equation of  $\varphi$  can be obtained as

$$10 \quad \varphi = \frac{(f_{ps} - f_{pe}) L}{E_p \epsilon_{cu} d_p [1 - (A_p f_{ps} + A_s f_y - A'_s f'_y - C_f) / (0.85 \beta_1 f'_c b_w d_p)]}$$

The tendon stress at ultimate  $f_{ps}$  can be obtained by rearranging Equation 10 as

$$11a \quad \begin{aligned} f_{ps} &= f_{pe} + \Delta f_{ps} = f_{pe} \\ &+ \frac{\varphi E_p \epsilon_{cu} (d_p - c_{pe})}{L} / \left( 1 + \frac{\varphi E_p A_p \epsilon_{cu}}{0.85 \beta_1 f'_c b_w L} \right) \quad (\text{MPa}) \end{aligned}$$

$$11b \quad c_{pe} = \frac{A_p f_{pe} + A_s f_y - A'_s f'_y - C_f}{0.85 \beta_1 f'_c b_w} \quad (\text{mm})$$

$$11c \quad c = c_{pe} + \frac{A_p \Delta f_{ps}}{0.85 \beta_1 f'_c b_w} \quad (\text{mm})$$

$$11d \quad \begin{cases} C_f = 0.85 \beta_1 f'_c (b - b_w) h_f & \text{if } \beta_1 c > h_f \\ C_f = 0, \quad b_w = b & \text{if } \beta_1 c \leq h_f \end{cases}$$

Assuming  $\epsilon_{cu} = 0.003$  and using the measured  $f_{ps}$  and  $c$  calculated from Equation 2, the values of  $\varphi$  can be obtained from Equation 10. Au and Du<sup>16</sup> found that  $\varphi$  tended to be constant in a series of 148 simply supported specimens, in which the mean, standard deviation and coefficient of variation of  $\varphi$  are 16.1, 6.8 and 0.42 respectively. Taking  $\varphi \cong 10$  is therefore considered as conservative in most cases of PC members with unbonded tendons. In their study, however, almost all unbonded tendons are made of steel. Whether the conclusion applies to FRP tendons needs further validation.

## 4. EVALUATION OF PARAMETER $\varphi$ BASED ON EXPERIMENTS

### 4.1. Experimental work by Au et al.<sup>2</sup> at The University of Hong Kong (HKU)

Two groups of simply supported UPPC beams, each having two external tendons, were tested to failure. Group S (i.e. SSS1 to SSS3) used 7-wire steel strands of 12.9 mm nominal diameter, while group P (i.e. PSS1 to PSS3) used AFRP tendons of 10.5 mm nominal core diameter. Figure 2

shows the dimensions of the specimens while its material properties and the measured ultimate tendon stress  $f_{ps}$  are shown in Table 1. The amounts of prestressing force, non-prestressed reinforcement and concrete strength of specimens in group S roughly correspond to those in group P. For convenience, the specimens were divided into three sub-groups each having roughly the same nominal partial prestressing ratio (PPR) defined as  $PPR = A_p f_{pe} / (A_p f_{pe} + A_s f_y)$ . Specimens SSS1 and PSS1 had nominal parameter  $PPR = 0.25$ . Specimens SSS2 and PSS2 had nominal parameter  $PPR = 0.3$ , while specimens SSS3 and PSS3 had nominal parameter  $PPR = 0.5$ .

Specimens SSS1, SSS2, PSS1 and PSS2 were cast of grade 60 concrete while specimens SSS3 and PSS3 were cast of grade 85 concrete. The actual cube strengths on the day of testing are shown in Table 1. The prestressing level of tendon, defined as the ratio of effective prestress  $f_{pe}$  to ultimate strength  $f_{pu}$ , of the specimens tested ranged from 18.2% to 25.8% for steel tendons and from 30.4% to 40.3% for AFRP tendons.

#### 4.2. Experimental work by Du<sup>1</sup> at Beijing Jiao Tong University (BJTU)

Four simply supported UPPC beams (i.e. B1 to B4) each with two external tendons were tested to failure under third-point

loading. Specimen B2 used 7-wire steel strands of 15.2 mm nominal diameter, while specimens B1, B3 and B4 used CFRP tendons. Each tendon consisted of three CFRP bars of 7 mm diameter and nominal tensile strength of 2400 MPa. The reinforcement was characterised by the combined reinforcement index  $q_0$  at mid-span section defined as

$$q_0 = (A_p f_{pe} + A_s f_y) / (b d_p f'_c)$$

Specimens B1, B3 and B4 had nominal parameter  $q_0$  of 0.15, 0.20 and 0.25 respectively. The amounts of prestressing force, non-prestressed reinforcement and concrete strength of specimen B2 roughly correspond to those in specimen B3. Figure 3 shows the dimensions of the specimens, while the material properties and the measured ultimate tendon stress  $f_{ps}$  are shown in Table 2. The parameter PPR for specimens B1 to B4 is between 0.47 and 0.62.

#### 4.3. Experimental work by Ghallab and Beeby<sup>3</sup>

Sixteen PC beams with the same cross-section were tested under either mid-span or third-point loading up to failure after being strengthened using two external AFRP tendons with one or two deviators. Except for specimen PC12, all specimens were internally prestressed using a 7 mm diameter high tensile steel

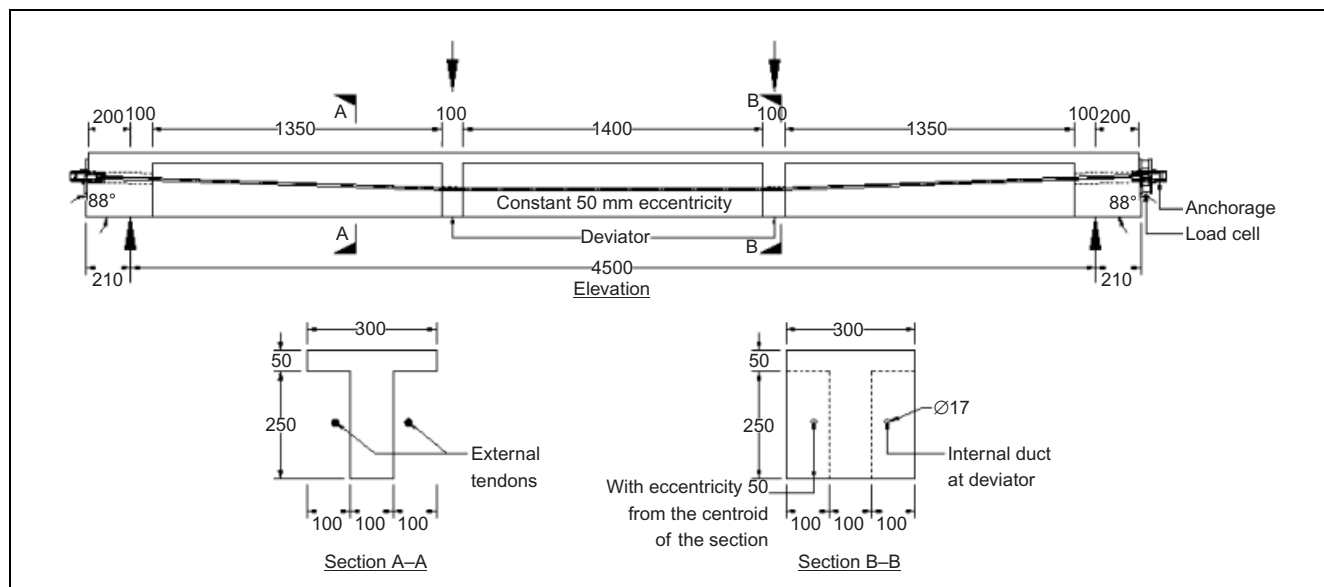


Figure 2. Dimensions of specimens by Au et al. at HKU (unit: mm)

No.	$L_n$ : mm	$L$ : mm	$f'_c$ : MPa	$A_s$ : mm <sup>2</sup>	$f_y$ : MPa	$A'_s$ : mm <sup>2</sup>	$f'_y$ : MPa	$A_p$ : mm <sup>2</sup>	$d_p$ : mm	$E_p$ : kN/mm <sup>2</sup>	$f_{pe}$ : MPa	$f_{ps}$ : MPa
SSS1	4500	5036	58.3	402	549.0	317.0	492.0	198	168.8	201.9	357.0	865.8
SSS2	4500	5036	49.2	402	549.0	317.0	492.0	198	168.8	201.9	505.0	996.9
SSS3	4500	5036	80.5	159	492.0	317.0	492.0	198	168.8	201.9	422.0	1013.4
PSS1	4500	5036	55.2	402	549.0	317.0	492.0	109	168.8	126.5	577.0	963.2
PSS2	4500	5036	44.8	402	549.0	317.0	492.0	109	168.8	126.5	766.0	1183.1
PSS3	4500	5036	79.6	159	492.0	317.0	492.0	109	168.8	126.5	709.0	1223.6
B1	3000	3200	42.2	308	344.5	226.1	371.1	231	231.5	142.0	663.1	1212.8
B2	3000	3200	38.5	402	382.9	226.1	371.1	280	307.7	197.0	864.6	1481.0
B3	3000	3200	41.0	402	382.9	226.1	371.1	231	231.5	142.0	717.1	1143.5
B4	3000	3200	44.7	509	362.2	226.1	371.1	231	231.5	142.0	702.5	1127.5

Table 1. Details of specimens by Au et al.<sup>2</sup> and Du<sup>1</sup>

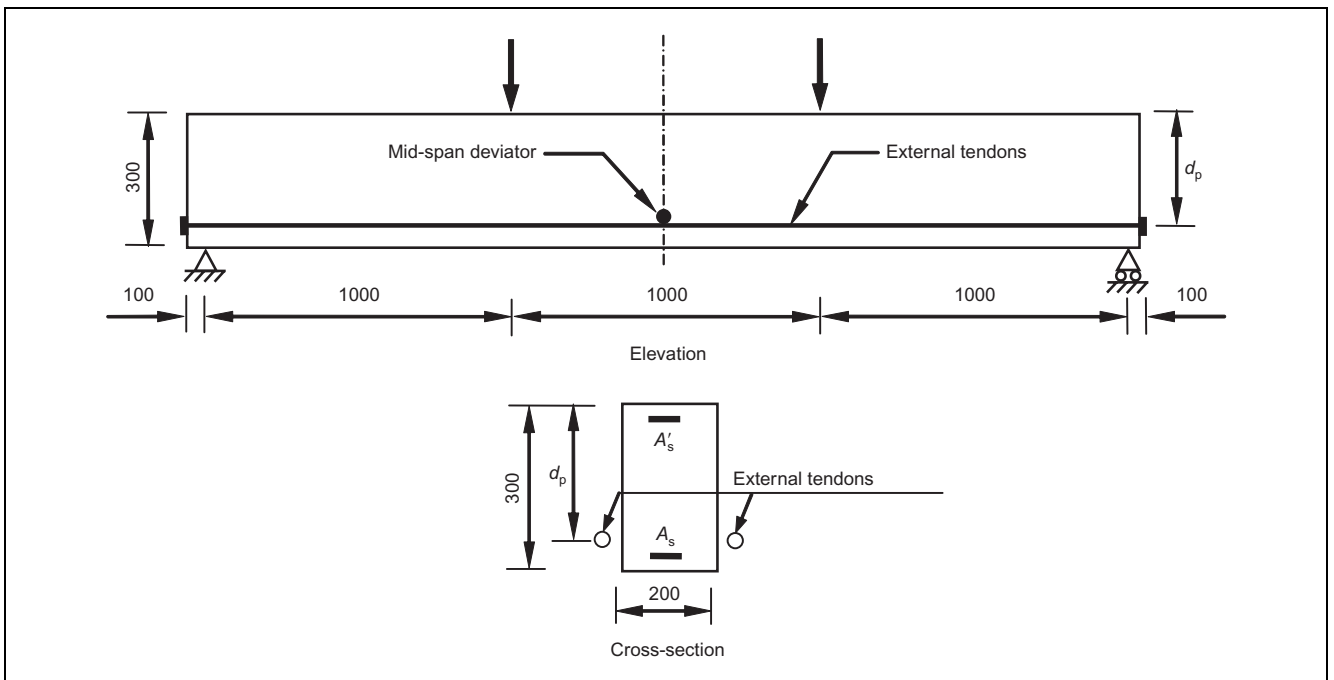


Figure 3. Dimensions of specimens by Du at BJTU (unit: mm)

No.	$L_n$ : mm	$L$ : mm	$f'_c$ : MPa	$A_s$ : mm <sup>2</sup>	$f_y$ : MPa	$A'_s$ (mm <sup>2</sup> )	$f'_y$ : MPa	$A_p$ : mm <sup>2</sup>	$d_p$ : mm	$E_p$ : kN/mm <sup>2</sup>	$f_{pe}$ : MPa	Internal prestressed steel area: mm <sup>2</sup>	Internal effective prestress: MPa
PC1	2592	2692	42.6	100.6	368	100.6	368	61.1	142.2	126.5	785.3	38.5	1008.8
PC2	2592	2692	44.6	100.6	368	100.6	368	61.1	142.2	126.5	987.7	38.5	931.4
PC3	2592	2692	44.0	100.6	368	100.6	368	61.1	142.2	126.5	1182.8	38.5	896.7
PC4	2592	2692	38.2	100.6	368	100.6	368	61.1	142.2	126.5	982.2	38.5	954.3
PC5	2592	2692	41.8	100.6	368	100.6	368	61.1	160.2	126.5	990.5	38.5	919.3
PC6	2592	2692	36.6	100.6	368	100.6	368	61.1	192.6	126.5	998.9	38.5	892.5
PC7	2592	2692	34.6	100.6	368	100.6	368	61.1	142.2	126.5	990.5	38.5	915.2
PC8	2592	2692	63.4	100.6	368	100.6	368	61.1	142.2	126.5	984.6	38.5	1003.0
PC9	3600	3700	39.0	100.6	368	100.6	368	61.1	142.2	126.5	988.0	38.5	967.0
PC10	1800	1900	38.0	100.6	368	100.6	368	61.1	142.2	126.5	994.0	38.5	1004.0
PC11	2592	2692	38.9	0.0	—	0.0	—	61.1	142.2	126.5	991.2	38.5	996.9
PC12	2592	2692	37.6	100.6	368	100.6	368	61.1	142.2	126.5	991.2	0.0	—
PC13	2592	2692	50.4	100.6	368	100.6	368	61.1	142.2	126.5	987.2	38.5	359.2
PC14	2592	2692	39.7	100.6	368	100.6	368	61.1	142.2	126.5	998.9	38.5	968.8
PC15	2592	2692	37.6	100.6	368	100.6	368	61.1	142.2	126.5	984.5	38.5	956.6
PC16	2592	2692	35.1	100.6	368	100.6	368	61.1	142.2	126.5	814.2	38.5	961.3

Table 2. Details of specimens by Ghallab and Beeby<sup>3</sup>

wire with yield strength of 1470 MPa about one week after casting. The experiment was carried out to study the effect of several factors on the ultimate stress in external AFRP tendons, including the ratio of effective stress to ultimate tendon strength  $f_{pe}/f_{pu}$ , depth to external tendons  $d_p$ , number of deviators, ratio of distance between deviators to the span length, concrete strength, span/depth ratio, ratio of internal bonded prestressed steel to non-prestressed steel, and the load type. Figure 4 shows the dimensions of the specimens, with their material properties shown in Table 3. The parameter PPR for specimens PC1 to PC12 is between 0.74 and 1.00.

#### 4.4. Evaluation of parameter $\phi$

The parameter  $\phi$  is further studied for UPPC members mainly with FRP tendons. In using Equation 10,  $\epsilon_{cu}$  is taken as 0.003, and the other parameters have adopted the specific values as

listed in Tables 1 and 2. The total length of specimen or the length of tendon between anchorages  $L$  is adopted but not the net span  $L_n$ . As the Young's modulus of tendons affects  $\phi$ , the values of  $\phi$  of specimens with FRP tendons are converted to those of the corresponding specimens with steel tendons for comparison on the same basis. In the conversion, the right side of Equation 10 for specimens with FRP tendons is divided by  $\lambda = E_{steel}/E_{FRP}$ , where  $E_{steel}$  and  $E_{FRP}$  are Young's moduli of steel and FRP tendons, respectively. The values of  $\phi$  for each specimen before and after conversion are calculated for the above sets of experimental results and shown in Table 3.

In the tests of Au *et al.*,<sup>2</sup> the mean, standard deviation and coefficient of variation of  $\phi$  are respectively 37.9, 3.71 and 0.10 for the three specimens with AFRP tendons before conversion. After conversion they are 26.9, 3.60 and 0.13,

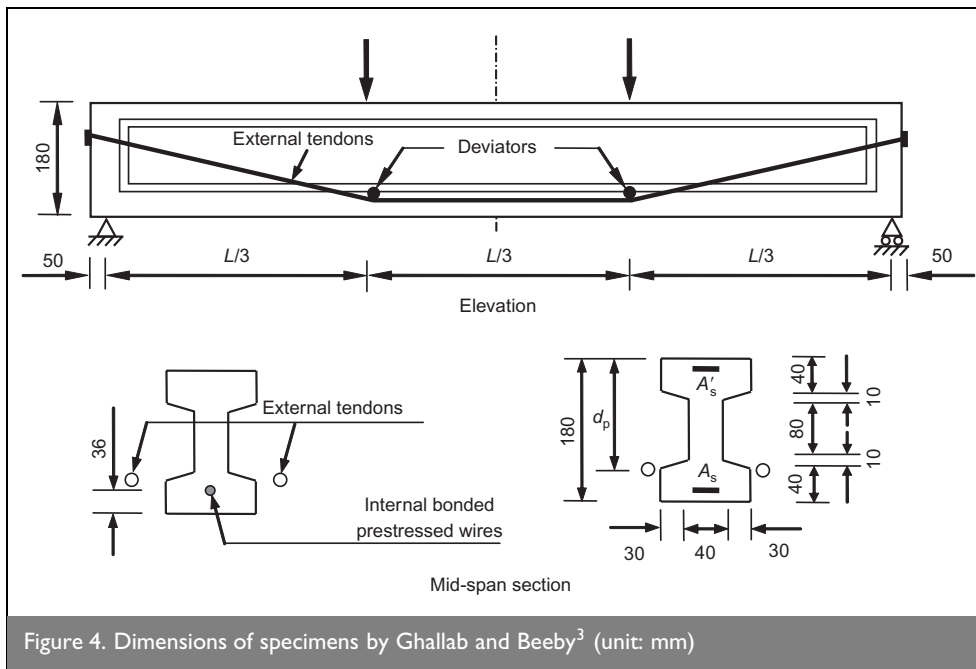


Figure 4. Dimensions of specimens by Ghallab and Beeby<sup>3</sup> (unit: mm)

No.	Tendon materials	$\phi$ before conversion	$\phi$ after conversion	No.	Tendon materials	$\phi$ before conversion	$\phi$ after conversion
SSS1	Steel	29.3	29.3	PC4	AFRP	15.7	10.0
SSS2	Steel	29.5	29.5	PC5	AFRP	25.2	16.0
SSS3	Steel	30.8	30.8	PC6	AFRP	23.9	15.1
PSS1	AFRP	34.1	21.6	PC7	AFRP	26.4	16.7
PSS2	AFRP	38.0	24.1	PC8	AFRP	37.9	24.0
PSS3	AFRP	41.5	26.3	PC9	AFRP	33.3	21.1
B1	CFRP	23.6	16.7	PC10	AFRP	19.6	12.4
B2	Steel	15.7	15.7	PC11	AFRP	27.3	17.3
B3	CFRP	19.0	13.5	PC12	AFRP	21.3	13.5
B4	CFRP	19.2	13.6	PC13	AFRP	23.8	15.0
PC1	AFRP	23.9	15.2	PC14	AFRP	12.1	7.7
PC2	AFRP	27.9	17.7	PC15	AFRP	25.5	16.1
PC3	AFRP	18.1	11.5	PC16	AFRP	—	—

Table 3. Value of  $\phi$  before and after conversion

respectively, for all six specimens. In the tests of Du,<sup>1</sup> the mean, standard deviation and coefficient of variation of  $\phi$  are respectively 20.6, 2.58 and 0.13 for the three specimens with CFRP tendons before conversion. After conversion they are 14.9, 1.59 and 0.11, respectively, for all four specimens. In the tests of Ghallab and Beeby,<sup>3</sup> the mean, standard deviation and coefficient of variation of  $\phi$  are respectively 24.1, 6.47 and 0.27 for all 15 specimens with AFRP tendons before conversion. After conversion, they are 15.3, 4.09 and 0.27, respectively. In the 25 specimens from the three groups, the mean, standard deviation and coefficient of variation of  $\phi$  are respectively 18.0, 6.23 and 0.35 after conversion. The statistics for 25 specimens are comparable to the 148 specimens studied by Au and Du,<sup>16</sup> in which the mean, standard deviation and coefficient of variation of  $\phi$  are 16.1, 6.8 and 0.42, respectively.

Despite minor variations, the values of  $\phi$  are generally stable and tend to be constant in tests having tendons of the same materials. As pointed out by Au and Du,<sup>16</sup> the difference in measurement methods, failure criteria adopted, and variation of material properties may have caused the scatter of results. The

difference between the total length of specimen  $L$  and the net span  $L_n$  used by different investigators also have some effect on the variation of  $\phi$ . For example, the tests of Au *et al.*<sup>2</sup> had  $L/L_n$  as large as 1.12, while those of Du<sup>1</sup> had  $L/L_n$  of 1.07. The tests of Ghallab and Beeby<sup>3</sup> had  $L/L_n$  of only 1.04 or less. After rearranging the right side of Equation 10, Au and Du<sup>16</sup> qualitatively explained why the parameter  $\phi$  could be constant. Hence it is reasonable to take  $\phi$  as a constant in PC members with unbonded FRP tendons. The parameter  $\phi_{FRP}$  for specimens with FRP tendons can be expressed as

$$\phi_{FRP} = \lambda \phi_{steel}$$

where  $\phi_{steel}$  is the parameter  $\phi$  for specimens with steel tendons.

As taking the value of  $\phi_{steel}$  around 10 is conservative in most cases,<sup>16</sup>  $\phi_{steel} = 10$  is suggested here for regular design purposes. In Table 3, it can also be found that only one of the values of  $\phi$  is less than 10 after the conversion from FRP to steel. Figure 5 compares the values of  $\phi$  for the above-

mentioned 25 specimens after conversion against the rule of  $\varphi_{\text{steel}} = 10$ . Equation 13 shows that if Young's modulus of FRP is less than that of steel,  $\varphi_{\text{FRP}}$  is larger than  $\varphi_{\text{steel}}$  and vice versa. As the parameter  $\varphi$  is directly related to the equivalent plastic hinge length  $L_p$  and ultimate tendon stress  $f_{ps}$ , the influence of Young's moduli of FRP and steel tendons on  $L_p$ , and hence on  $f_{ps}$  would be roughly the same as that on the parameter  $\varphi$ .

### 5. PROPOSED EQUATION FOR ULTIMATE STRESS IN EXTERNAL TENDONS

With the determination of  $\varphi_{\text{FRP}}$  and substituting  $\varphi_{\text{FRP}} = 10\lambda$  and  $\epsilon_{\text{cu}} = 0.003$  into Equation 8, the ultimate stress in external FRP tendons can be expressed as

$$14 \quad f_{ps} = f_{pe} + \frac{0.03\lambda E_{\text{FRP}}(d_p - c)}{l_e} \leq (f_{pu})_{\text{FRP}} \quad (\text{MPa})$$

where  $(f_{pu})_{\text{FRP}}$  is the ultimate tensile strength of FRP tendons,  $\lambda = E_{\text{steel}}/E_{\text{FRP}}$ ,  $l_e = L/(1 + N/2)$ , and  $N$  is the number of support hinges required to form a failure mechanism crossed by the tendon. The practice of AASHTO LRFD Code<sup>12</sup> for continuous beams is adopted because some investigation<sup>17</sup> showed that the rotation at a supported plastic hinge was only half of that at a mid-span plastic hinge in some cases. It means that the equivalent plastic hinge length at an interior support is half of that at mid-span in continuous beams.

In Equation 14,  $0.03\lambda E_{\text{FRP}}(d_p - c)$  is actually equal to  $0.03 E_{\text{steel}}(d_p - c)$  or  $6000 (d_p - c)$  that is independent of  $E_{\text{FRP}}$ . It shows that Pannell's deformation-based design equations can predict the ultimate stress in unbonded FRP tendons, although they have been established for unbonded steel tendons without explicitly including their Young's moduli. Ghallab and Beeby<sup>3</sup> experimentally found that the equation in BS 8110 generally gave good agreement with the actual results for AFRP tendons after changing the limit of  $f_{ps} \leq 0.7 f_{pu}$  for steel to  $f_{ps} \leq (f_{pu})_{\text{FRP}}$  for FRP. The present systematic analysis of experimental data from various sources shows that Equation 14 can be rewritten in a unified form as

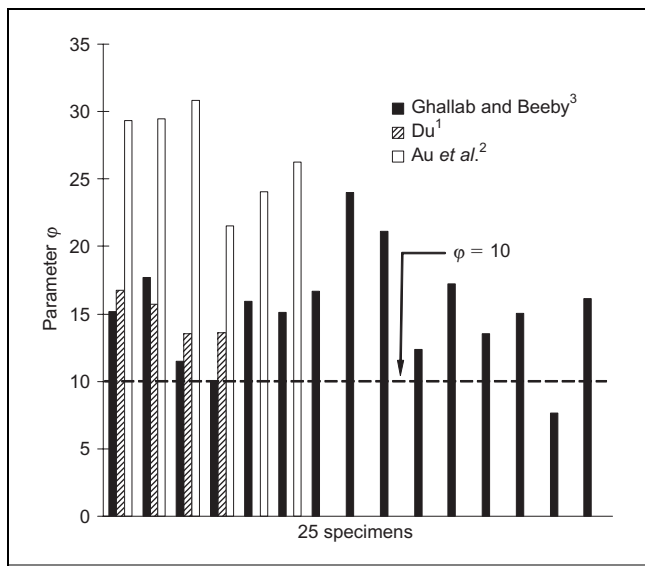


Figure 5. Comparison of parameter  $\varphi$  for 25 specimens after conversion from FRP to steel

$$15 \quad f_{ps} = f_{pe} + \frac{6000 (d_p - c)}{l_e} \leq (f_{pu})_{\text{FRP}} \text{ or } (f_{py})_{\text{steel}} \quad (\text{MPa})$$

where the neutral axis depth  $c$  can be solved from Equations 2a to 2c for section equilibrium,  $l_e = L/(1 + N/2)$ ,  $L$  is the length of tendon between anchorages or fully bonded deviators, and  $N$  is the number of support hinges required to form a failure mechanism crossed by the tendon in continuous beams.

To demonstrate the validity of Equation 15, the computed values of tendon stress  $f_{ps}$  at ultimate are compared with the above experimental results, and the results of correlation analyses are plotted in Figure 6 giving a correlation coefficient of 0.89. Most of the predicted values of tendon stress  $f_{ps}$  at ultimate are on the safe side. Note that Equation 15 is similar in form to the AASHTO equation (i.e. Equation 9) except that the use of  $\varphi = 10.5$  resulting in a higher coefficient 6300 will be slightly less safe in view of the experimental results.

The unbonded tendon stresses  $f_{ps}$  at ultimate are also computed for the above specimens using the equation in the ACI 318-08 building code,<sup>24</sup> namely

$$16 \quad f_{ps} = f_{pe} + 70 + \frac{f'_c}{\lambda \rho_p} \quad (\text{MPa})$$

where  $\rho_p = A_p/bd_p$ ; for span-to-depth ratio  $L_n/d_p$  of 35 or less,  $\lambda=100$ , and  $f_{ps}$  shall not be taken as greater than the lesser of  $f_{py}$  and  $(f_{pe} + 420)$ ; for  $L_n/d_p$  greater than 35,  $\lambda = 300$ , and  $f_{ps}$  shall not be taken as greater than the lesser of  $f_{py}$  and  $(f_{pe} + 210)$ . Figure 7 plots the computed values of  $f_{ps}$  using Equation 16 against the experimental results, giving a correlation coefficient of 0.80. For these specimens, the correlation coefficient based on the ACI 318-08 building code is less than that based on Equation 15.

### 6. CONCLUSIONS

This paper has evaluated the validation of Pannell's deformation-based method to predict the ultimate stress in FRP tendons of UPPC beams. The ratio  $\varphi$  of equivalent plastic hinge

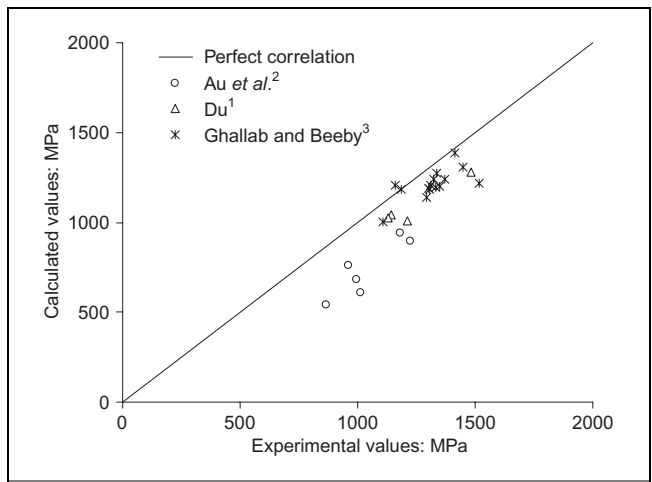


Figure 6. Comparison of calculated value of  $f_{ps}$  based on Equation 15 against experimental values

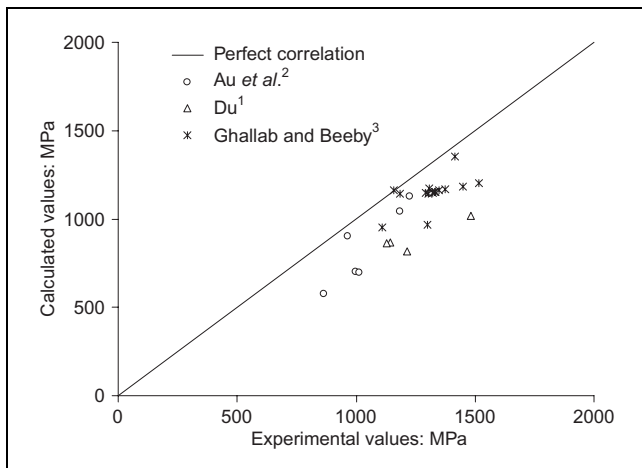


Figure 7. Comparison of calculated values of  $f_{ps}$  based on equation 16 against experimental values

length to neutral axis depth at critical section is analysed based on the experimental results from three research groups. The parameter  $\phi$  can be regarded as a constant for UPPC members with FRP tendons but it is also related to the Young's modulus of FRP. A modified equation similar in form to those adopted by various design codes is proposed, and it is applicable to both FRP and steel tendons.

#### ACKNOWLEDGEMENT

The work described in this paper has been supported by the Research Grants Council of the Hong Kong Special Administrative Region, China (RGC Project No. HKU 7101/04E).

#### REFERENCES

1. DU J. S. *Experimental Study of Partially Prestressed Concrete Beams with External CFRP Tendons*. School of Civil Engineering, Beijing Jiao Tong University, Beijing, 2007, Research report (in Chinese).
2. AU F. T. K., SU R. K. L., TSO K. and CHAN K. H. E. Behaviour of partially prestressed concrete beams with external tendons. *Magazine of Concrete Research*, 2008, 60, No. 6, 455–467.
3. GHALLAB A. and BEEBY A. W. Factors affecting the external prestressing stress in externally strengthened prestressed concrete beams. *Cement and Concrete Composites*, 2005, 27, No. 9–10, 945–957.
4. NAAMAN A. E. and ALKHAIRI F. M. Stress at unbonded post-tensioned tendons: Part 1 – evaluation of the state-of-the-art. *ACI Structural Journal*, 1991, 88, No. 5, 641–651.
5. ALLOUCHE E. N., CAMPBELL T. I., GREEN M. F. and SOUDKI K. A. Tendon stress in continuous unbonded prestressed concrete members. Part 1: review of literature. *PCI Journal*, 1998, 43, No. 6, 86–93.
6. AU F. T. K. and DU J. S. Partially prestressed concrete. *Progress in Structural Engineering and Materials*, 2004, 6, No. 2, 127–135.
7. NAAMAN A. E. and ALKHAIRI F. M. Stress at ultimate in unbonded post-tensioned tendons. Part 2: proposed methodology. *ACI Structural Journal*, 1991, 88, No. 6, 683–692.

8. NAAMAN A. E., BURNS N., FRENCH C., GAMBLE W. L. and MATTOCK A. H. Stresses in unbonded prestressing tendons at ultimate: Recommendation. *ACI Structural Journal*, 2002, 99, No. 4, 518–529.
9. GHALLAB A. and BEEBY A. W. Ultimate strength of externally-strengthened prestressed beams. *Proceedings of the Institution of Civil Engineers: Structures and Buildings*, 2002, 152, No. 4, 395–406.
10. NG C. K. Tendon stress and flexural strength of externally prestressed beams. *ACI Structural Journal*, 2003, 100, No. 5, 644–653.
11. AMERICAN ASSOCIATION OF STATE HIGHWAY AND TRANSPORTATION OFFICIALS. *AASHTO LRFD Bridge Design Specification*. SI Unit 1st edn. AASHTO, Washington, 1994.
12. AMERICAN ASSOCIATION OF STATE HIGHWAY AND TRANSPORTATION OFFICIALS. *AASHTO LRFD Bridge Design Specifications*. SI Unit. AASHTO, Washington, 1998.
13. HARAJLI M. H. Effect of span–depth ratio on the ultimate steel stress in unbonded prestressed concrete members. *ACI Structural Journal*, 1990, 87, No. 3, 305–312.
14. PANNELL F. N. The ultimate moment of resistance of unbonded prestressed concrete beams. *Magazine of Concrete Research*, 1969, 21, No. 66, 43–54.
15. TAM A. and PANNELL F. N. Ultimate moment of resistance of unbonded partially prestressed reinforced concrete beams. *Magazine of Concrete Research*, 1976, 28, No. 97, 203–208.
16. AU F. T. K. and DU J. S. Prediction of ultimate stress in unbonded prestressed tendons. *Magazine of Concrete Research*, 2004, 56, No. 1, 1–11.
17. ROBERTS-WOLLMANN C. L., KREGER M. E., ROGOWSKY D. M. and BREEN J. E. Stresses in external tendons at ultimate. *ACI Structural Journal*, 2005, 102, No. 2, 206–213.
18. AMERICAN ASSOCIATION OF STATE HIGHWAY AND TRANSPORTATION OFFICIALS. *Guide Specifications for Design and Construction of Segmental Concrete Bridges*, 2nd edn. AASHTO, Washington, 1999.
19. HARAJLI M. H. On the stress in unbonded tendons at ultimate: critical assessment and proposed changes. *ACI Structural Journal*, 2006, 103, No. 6, 803–812.
20. HARAJLI M. H. and KANJ M. Y. Ultimate flexural strength of concrete members prestressed with unbonded tendons. *ACI Structural Journal*, 1991, 88, No. 6, 663–673.
21. BRITISH STANDARDS INSTITUTION. *Structure Use of Concrete*. BSI, London, 1985, BS 8110—Parts 1, 2 and 3.
22. CANADIAN STANDARDS ASSOCIATION. *Design of Concrete Structures (A23.3-94)*. CSA, Rexdale, Ontario, Canada, 1994.
23. LIU S. L. and DU J. S. Proposed equation for ultimate stress in external tendons in practical engineering design. *Prestressing Technology*, 2006, No. 3, 22–25 (in Chinese).
24. AMERICAN CONCRETE INSTITUTE. *Building Code Requirements for Structural Concrete (ACI 318-08) and Commentary*. ACI, Farmington Hills, Michigan, USA, 2008. ACI Committee 318.

#### What do you think?

To comment on this paper, please email up to 500 words to the editor at [journals@ice.org.uk](mailto:journals@ice.org.uk)

*Proceedings* journals rely entirely on contributions sent in by civil engineers and related professionals, academics and students. Papers should be 2000–5000 words long, with adequate illustrations and references. Please visit [www.thomastelford.com/journals](http://www.thomastelford.com/journals) for author guidelines and further details.